

# Bubble-Up: Increasing Utilization in Modern Warehouse Scale Computers via Sensible Co-locations

Jason Mars  
University of Virginia  
jom5x@cs.virginia.edu

Lingjia Tang  
University of Virginia  
lt8f@cs.virginia.edu

Robert Hundt  
Google  
rhundt@google.com

Kevin Skadron  
University of Virginia  
skadron@cs.virginia.edu

Mary Lou Soffa  
University of Virginia  
soffa@cs.virginia.edu

## ABSTRACT

As much of the world’s computing continues to move into the cloud, the overprovisioning of computing resources to ensure the performance isolation of *latency-sensitive* tasks, such as web search, in modern datacenters is a major contributor to low machine utilization. Being unable to accurately predict performance degradation due to contention for shared resources on multicore systems has led to the heavy handed approach of simply disallowing the co-location of high-priority, latency-sensitive tasks with other tasks. Performing this *precise* prediction has been a challenging and unsolved problem.

In this paper, we present **Bubble-Up**, a characterization methodology that enables the accurate prediction of the performance degradation that results from contention for shared resources in the memory subsystem. By using a *bubble* to apply a tunable amount of “pressure” to the memory subsystem on processors in production datacenters, our methodology can predict the performance interference between co-locate applications with an accuracy within 1% to 2% of the actual performance degradation. Using this methodology to arrive at “sensible” co-locations in Google’s production datacenters with real-world large-scale applications, we can improve the utilization of a 500-machine cluster by 50% to 90% while guaranteeing a high quality of service of latency-sensitive applications.

## Categories and Subject Descriptors

B.3.3 [Hardware]: Memory Structures—*Performance Analysis and Design Aids*; C.4 [Computer Systems Organization]: Performance of Systems—*Design studies*; D.4.8 [Operating Systems]: Performance—*measurements, monitors*

## General Terms

Design, Performance, Measurement

Permission to make digital or hard copies of all or part of this work for personal or classroom use is granted without fee provided that copies are not made or distributed for profit or commercial advantage and that copies bear this notice and the full citation on the first page. To copy otherwise, to republish, to post on servers or to redistribute to lists, requires prior specific permission and/or a fee.

MICRO’11, December 3–7, 2011, Porto Alegre, Brazil.

Copyright 2011 ACM 978-1-4503-1053-6/11/12 ...\$10.00.

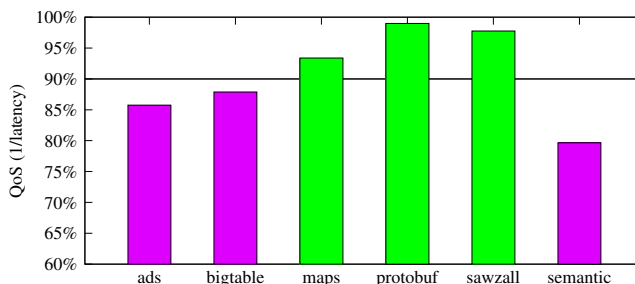


**Figure 1:** Some co-locations violate web search’s 90% QoS threshold. The inability to precisely predict this performance interference leads to disallowing co-location for web search and consequently, low machine utilization.

## 1. INTRODUCTION

“Warehouse scale computers” (WSCs) [12, 22] house large scale web applications and cloud services. The cost of construction and operation of these datacenters ranges from tens to hundreds of millions of dollars. As more computing moves into the cloud, it is becoming exceedingly important to leverage the resources in WSCs as efficiently as possible. However, the utilization of the computing resources in modern WSCs remains low, often not exceeding 20% [2].

Each machine in the datacenter house numerous cores, often 4 to 8 cores per socket, and 2 to 4 sockets per machine. However, in light of the significant potential for parallelism on a single machine, there are a number of resources shared among cores. This sharing can result in performance interference across-cores, negatively and unpredictably impacting the quality of service (QoS) of user-facing and latency-sensitive application threads [36]. To avoid the potential for interference, co-location is disallowed for latency-sensitive applications, leaving cores idle, and resulting in an overprovisioning that negatively impacts the utilization of the entire datacenter.

This overprovisioning is often unnecessary, as co-locations may or may not result in significant performance interference. Figure 1 demonstrates this uncertainty. In this figure, we show the performance ( $\frac{1}{latency}$ ), normalized to solo execution, of a key user-facing component of Google’s web search when co-located with other Google workloads on a single socket. The horizontal line shows the maximum allowable performance interference. The co-location of some

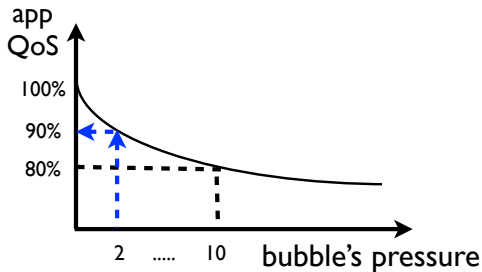


**Figure 2: Example sensitivity curve for *A*. Assuming *B*’s pressure score is 2 we can predict *A* will be performing at 90% of full performance.**

workloads does not violate this QoS threshold (light bars), while others violate the threshold (dark bars). An inability to *precisely* predict the performance impact for a given co-location leads to the heavy handed solution of simply disallowing co-location. On the other hand, without prediction, profiling all possible co-locations’ performance interference beforehand to guide co-location decisions is prohibitively expensive. The profiling complexity for all pairwise co-locations is  $O(N^2)$  ( $N$  as the number of applications). With hundreds to thousands of applications running in a datacenter, and the frequent development and updating of these applications, a brute-force profiling approach is not practical.

The goal of this work is to enable the *precise* prediction of the performance degradation that results from contention for shared resources in the memory subsystem. A *precise* prediction is one that provides an expected amount of performance lost when co-located. With this information, co-locations that do not violate the QoS threshold of an application can be allowed, resulting in improved utilization in the datacenter.

This is a challenging problem. The most relevant related work aims to classify applications based on how aggressive they are for the shared memory resources and identify co-locations to reduce contention based on the classification [3, 16, 17, 21, 23, 24, 37, 39, 41]. However prior work has not presented a solution to precisely predict the amount of performance degradation suffered by each application due to co-location, which is essential for co-location decisions of latency-sensitive applications in WSCs. In this work, we present such a solution: The **Bubble-Up** methodology.

The key insight of Bubble-Up is that predicting the performance interference of co-running applications can be decoupled into 1) measuring the pressure on the memory subsystem an application generates, and 2) measuring how much an application suffers from different levels of pressure. The underlying hypothesis is both pressure and sensitivity can be quantified using a common pressure metric. Having such a metric reduces the complexity of co-location analysis. As opposed to the brute force approach of profiling and characterizing every possible pairwise co-location, Bubble-Up only requires characterizing each application once to produce precise pairwise interference predictions (e.g.  $O(N)$ ).

Bubble-Up is a two-step characterization process. First, each application is tested against an expanding *bubble* to produce a *sensitivity curve*. The *bubble* is a carefully designed stress test for the memory subsystem that provides a “dial” for the amount of pressure applied to the entire

memory subsystem. This bubble is run along with the host application being characterized. As this dial is increased automatically (expanding the bubble), the impact on the host application is recorded, producing a sensitivity curve for the host application such as the one illustrated in Figure 2. On the y-axis, we have the normalized QoS performance of the application (latency, throughput, etc), and the x-axis shows the bubble pressure. In the second step, we identify a pressure score for the application using a *bubble pressure score reporter*. After these two steps of the Bubble-Up methodology is applied to each application, we have a sensitivity curve and a pressure score for each application. Given two applications *A* and *B*, we can then predict the performance impact of application *A* when co-located with application *B* by using *A*’s sensitivity curve to look up the relative performance of *A*, at *B*’s pressure score. In the example shown in Figure 2, *B* has a pressure score of 2, and as we can see from *A*’s sensitivity curve, *A*’s predicted QoS with that co-location is 90%.

The specific contributions of this work are as follows:

- We present the design of **Bubble-Up**, a general characterization methodology that enables the *precise* prediction of the performance degradation suffered by arbitrary applications when co-located.
- We introduce 17 production Google workloads and characterize their propensity to performance interference when co-located on production servers.
- In addition to demonstrating the prediction accuracy of our Bubble-Up methodology on the spectrum of contentious kernel in our **SmashBench** suite, we also evaluate the prediction accuracy and the improvement in utilization when applying the Bubble-Up methodology to steer pairwise co-locations of Google applications in a production datacenter environment.

Using Bubble-Up, we are able to precisely predict the performance degradation due to arbitrary co-locations of Google applications with at most a 2.2% error and often less than 1%. To evaluate using Bubble-Up to steer QoS enforced co-locations of production workloads, we perform a study in a 500-machine cluster and are able to increase the machine utilization in the cluster by 50%–90%, depending on the latency-sensitive applications’ allowable QoS threshold.

## 2. BACKGROUND

In this section, we describe how large-scale web-services are run in modern datacenters. We then discuss QoS and co-locations in production datacenters.

### 2.1 Datacenter Task Placement

In modern warehouse scale computers, each *web-service* is composed of one to hundreds of application *tasks*, and each task runs on a single machine. A *task* is composed of an application binary, associated data, and a configuration file that specifies the machine level resources required. These resources include the number of cores, amount of memory, and disk space that are to be allocated to the task. The configuration file for a tasks may also include special rules for the cluster manager such as whether to disallow co-locations with other tasks.

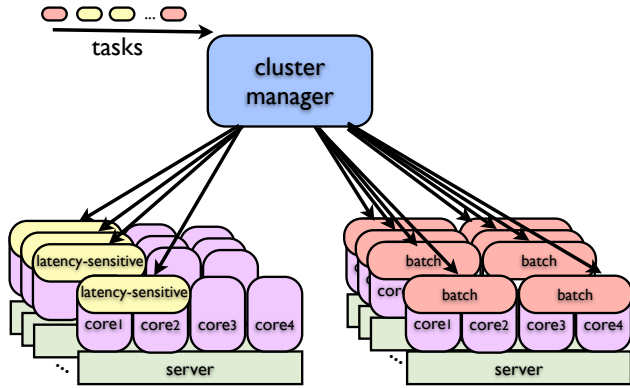


**Figure 3: Task placement in a cluster. The cluster manager does not co-locate latency-sensitive applications with others to protect their QoS from performance interference, causing low machine utilization.**

*Task placement* is conducted by a cluster-level manager that is responsible for a number of servers. Based on the resource requirement, the cluster manager uses an algorithm similar to bin-packing to place each task in a cluster of machines [25]. After a task is assigned a machine, a machine level manager (in the form of a daemon running in user-mode) uses *resource containers* [1] to allocate and manage the resources belonging to the task. For the remainder of this work, we use the term *application* to represent the program binary for a given component of a web-service, and *application task* as this binary coupled with its execution configuration file.

## 2.2 QoS and Co-location

### 2.2.1 Application QoS

As multicores become widely adopted in datacenters, the cluster manager consolidates multiple disparate tasks on a single server to improve the machine utilization. However, various application tasks in a datacenter often have different quality-of-service (QoS) priorities. User-facing applications for web search, maps, email and other internet services are *latency-sensitive*, and have high QoS priorities. Applications such as file backup, offline image processing, and video compression are *batch* applications that often have no QoS constraints. For these, latency is not as important. We define the QoS of a latency-sensitive application in terms of the relevant performance metric specified in its internal service level requirements (SLAs). For example, the QoS of Google’s web search is measured using query latency and queries-per-second, in contrast to Bing’s [15, 18], which uses the quality of search results provided. More details and examples are presented in Section 4.

### 2.2.2 QoS Flexibility

As discussed above, there is a trade-off between the QoS performance of latency-sensitive applications and the machine utilization in datacenters. When equipped with a precise prediction, we can allow a small amount of QoS degradation from co-location to improve the machine utilization. As long as a co-location pair is predicted to cause only a small amount of QoS degradation within a specified threshold, the cluster manager can allow the co-location. We specify the

tolerable amount of QoS degradation in a *QoS policy*. For example, a 95% QoS policy indicates that we are willing to sacrifice 5% of the QoS performance to improve machine utilization. To enforce these QoS policies, the precise prediction for QoS degradation due to co-location is needed.

### 2.2.3 Co-location

A simplified illustration of the task placement process is shown in Figure 3. The amount of required core and memory resources specified in the configuration of each task are carefully tuned by the developers of that task to achieve the QoS requirements. Latency-sensitive tasks that disallow co-location inadvertently occupies more resources on a server leading to unnecessary overprovisioning and lower machine utilization.

## 3. THE BUBBLE-UP METHODOLOGY

The key insight of Bubble-Up is that predicting the performance interference of co-running applications can be decoupled into two steps, 1) measuring how much an application suffers from different levels of pressure on the shared memory subsystem; and 2) measuring the pressure on the memory subsystem an application generates.

### 3.1 Two Step Methodology

Figure 4 illustrates the Bubble-Up methodology. The two steps to Bubble-Up are,

1. In Step 1, we characterize the *sensitivity* of each application task to pressure in the memory subsystem. In this step, we use a carefully designed stress test we call the *bubble* to iteratively increase the amount of pressure applied to the memory subsystem (e.g. bubble up in the subsystem). As we incrementally increase this pressure “dial”, we produce what we call a *sensitivity curve* for the application with QoS on the y-axis and pressure on the x-axis. This sensitivity curve shows how each application’s QoS degrades as pressure increases.
2. In Step 2, we characterize the *contentiousness* of each application task in terms of its pressure on the memory subsystem. We call this measure of contentiousness a *bubble score*. To identify the bubble score of an application, we use a *reporter* which observes how its own performance is affected by the application to generate a score for the application.

With the sensitivity curves and bubble scores of each application we are able to precisely predict the performance degradation from arbitrary co-locations. It is important to note that step one needs only to be applied to applications whose QoS needs to be enforced. Step two only needs to be applied to the applications that may threaten an application’s QoS.

### 3.2 Modeling Bubble-Up and Error

In this section, we present the formal modeling of our Bubble-Up methodology and the source of errors. We first provide a general model the performance degradation an application  $A$  suffers when co-running with other applications as,

$$Deg_{AC} = \sum_i^N (S_{AR_i} \times P_{CR_i}) \quad (1)$$

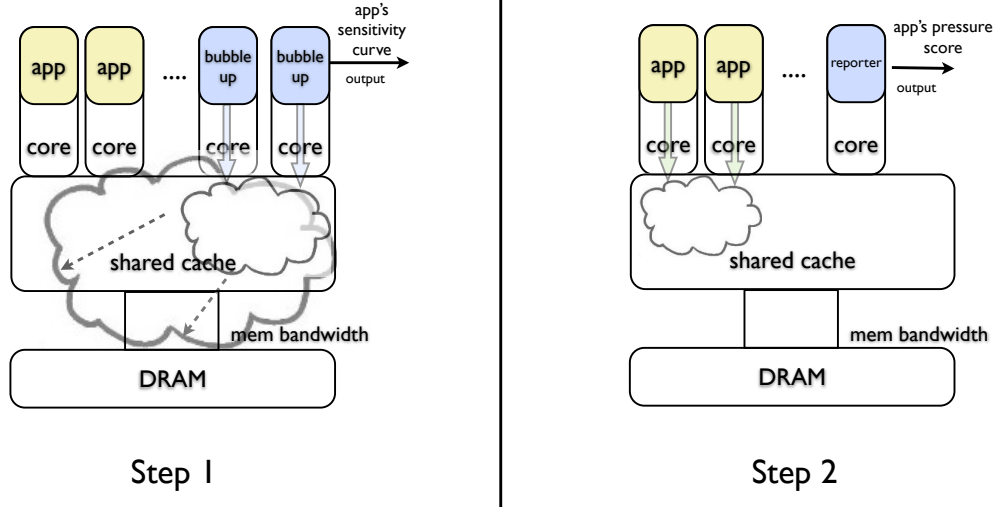


**Figure 4: Bubble-Up Methodology.** In Step 1, we characterize the *sensitivity* of the host application task to pressure in the memory subsystem using a *bubble*. In Step 2, we characterize the *contentiousness* of the host application in terms of the amount of pressure it causes on a *reporter*.

where  $A$  is the application,  $C$  is the co-runner or set of co-runners,  $Deg_{AC}$  is the  $A$ 's degradation when running with  $C$ ,  $R_i$  is a shared memory resource component such as shared cache, memory bandwidth or memory controller,  $P_{CR_i}$  is the pressure  $C$  generates on the shared resource  $R_i$ , and  $S_{AR_i}$  is  $A$ 's performance sensitivity to the pressure on the shared resource  $R_i$ . The total degradation is the sum of the stalled cycles caused by contention for each shared resource.

The main component of the Bubble-Up methodology is an expandable bubble, which functions as a “dial” for pressure on the memory system. We denote the bubble dial levels as a set  $B : \{B_0, B_1, \dots, B_M\}$  where  $M$  is the number of dial levels for the bubble. As we dial up, the bubble generates an increasing amount of pressure on each shared resource  $R_i$ , denoted as  $P_{B_j R_i}$ . In step 1 of Bubble-Up, we increase the bubble size and at each bubble dial  $j$ , we measure the degradation of application  $A$  when co-running with the bubble  $B_j$ . The result is a set of  $A$ 's degradations at varying bubble sizes:  $\{Deg_{AB_0}, Deg_{AB_1}, \dots, Deg_{AB_M}\}$ . This set is the discretized sensitivity curve of application  $A$ .

When the bubble reporter provides a pressure score of a co-running application  $C$ , it reports this pressure in the form of a bubble dial level,  $B_K$ , that generates the closest amount of pressure as  $C$  (for details see Section 3.4). To approximate application  $A$ 's degradation when co-running with  $C$  ( $Deg_{AC}$ ), Bubble-Up then uses  $A$ 's degradation when running with bubble  $B_K$  ( $Deg_{AB_K}$ ).

Because the pressure score is using the bubble's pressure to approximate an application's pressure, Bubble-Up introduces a small amount of error when predicting the degradation of  $A$ . This error stems from the mismatch of the relative pressures applied to the various individual shared resources. As we discuss in Section 3.3, this mismatch is minimized by designing the bubble to prioritize those resources that act as first-order effects in the degradation to  $A$ . By substituting  $Deg_{AC}$  and  $Deg_{AB_K}$  using Equation 1, we can formally model the prediction error as:

$$Error = \left| Deg_{AC} - \widetilde{Deg}_{AC} \right| \quad (2)$$

$$= \left| Deg_{AC} - Deg_{AB_K} \right| \quad (3)$$

$$= \sum_i^N |S_{AR_i} \times P_{B_K R_i} - S_{AR_i} \times P_{CR_i}| \quad (4)$$

### 3.3 Step One: Characterizing Sensitivity

As described in Section 2.1, each task is configured to use a prescribed number of cores for the cluster level bin packing algorithm used to assign tasks to machines in the datacenter. This number is usually less than the number of cores available on a socket. The bubble is run on the remaining cores. It is important to understand that there is no *correct* design for the bubble. Each design needs only to approximate varying levels of pressure, and there may be many good designs. In this paper, we present one such design, and show that our single bubble design is effective across myriad application workloads and architectures. Keep in mind that there are a number of assumptions made about the architectures for which this type of bubble design is applicable. Most importantly we assume the microarchitecture uses shared last level caches, memory controller, and bandwidth to memory.

#### 3.3.1 The Art of Bubble Design

Although there may be many ways to design a bubble, to arrive at a good design that is not prone to error and imprecision, there is a set of key requirements and guidelines that apply generally to bubble design.

1. **Monotonic Curves** - As the bubble's pressure increases (turning the pressure “dial” up) the amount of performance interference should also increase monotonically. Assuming the host application task is sensitive to cross-core interference, higher amounts of pressure should result in worse performance.

```

// Super cheap rand using a linear feedback shift register
unsigned lfsr;
#define MASK 0xd0000001u
#define rand (lfsr = (lfsr >> 1) ^ (unsigned int) \
(0 - (lfsr & 1u) & MASK))

unsigned int footprint_size=0; //Size of footprint
unsigned int dump[100]; //Dumps (manual ssa)

#define r (rand%footprint_size)

```

Figure 5: Bubble’s LFSR number generator.

```

while(1)
{
  dump[0]+=data_chunk[r]++;
  dump[1]+=data_chunk[r]++;
  dump[2]+=data_chunk[r]++;
  ...
  dump[98]+=data_chunk[r]++;
  dump[99]+=data_chunk[r]++;
}

```

Figure 6: Manual SSA for no dependencies.

2. **Wide Dial Range** - The pressure dial should have a range that captures the contentiousness of all the application tasks of interest. It should start from essential no pressure, and incrementally increase pressure to a point close to the maximum possible pressure, or at least worse than the most contentious application task in the set.
3. **Broad Impact** - The bubble should be designed to apply pressure to the memory subsystem as a whole, not stressing a single component in the memory subsystem. However, keep in mind that, as mentioned in Section 3.2, error is introduced in the difference in component pressure relative to the host task’s sensitivity. This error is generally minimized if first-order effects are prioritized.

### 3.3.2 Designing the Bubble

The design principle of our bubble is to use working set size as our measure of pressure. For a given working set size, we perform memory operations in software to exercise that working set as aggressively as possible.

Our bubble is a multithreaded kernel that generates memory traffic using both loads and stores with a mixture of random and streaming accesses. The number of threads spawned is based on the configuration file of the task being characterized. The pressure “dial” we use is the working set size on which our kernel works. For example, a pressure size of 1 means our bubble will continuously smash a 1MB chunk of memory. As we increase the pressure, we increase our kernel’s working set size. This increases the amount of data being pumped through the memory subsystem, as computation is not the bottleneck. Figures 5 – 7 show the key design points for our bubble.

As shown in Figure 5, we use a *linear shift feedback register* (LFSR) based psuedo random number generator as opposed the `rand` function provided by the C standard library. Minimizing the amount of computation in between memory accesses is critical to maximize the activity applied to a particular footprint. Using the standard library incurs a significant amount of computation between random numbers. However, an LFSR implementation requires only a few cycles to arrive at the next random number on modern processors. In our LFSR implementation, we use a mask of

```

while(1)
{
  double *mid=bw_data+(bw_stream_size/2);
  for(int i=0; i<bw_stream_size/2; i++)
  {
    bw_data[i]=scalar*mid[i];
  }
  for(int i=0; i<bw_stream_size/2; i++)
  {
    mid[i]=scalar*bw_data[i];
  }
}

```

Figure 7: Streaming access for bandwidth.

0xd0000001u, which produces a *period* of  $2^{32}$  random numbers.

Figure 6 shows the random memory accesses used in our bubble. Here we have manually constructed a basic block of 100 memory operations that are in *single static assignment* form such that there are no dependencies in between operations. This basic block has a high level of instruction level parallelism to maximize the number of operations applied to the footprint of the kernel.

As Figure 7 shows, we also use a streaming access pattern in our bubble. This implementation is based on the scalar portion of the STREAM bandwidth stressing benchmark. Using this access pattern further stresses the bandwidth to memory, and also triggers the prefetcher, another shared resource at the level of the shared last level cache.

## 3.4 Step Two: Bubble Scoring

The second step of Bubble-Up is to produce a pressure score for an application task that describes what size of bubble is representative of that task. To detect this score we use a bubble score *reporter*. The reporter is a carefully designed single threaded workload that is sensitive to contention. Like the bubble, the reporter is only designed once and then can be used with myriad applications and architectures.

### 3.4.1 Designing the Reporter

The reporter’s own sensitivity to performance interference is used as a basis for reporting how its own performance has been affected by the pressure generated by a host application. The impact *felt* by the reporter is then translated in terms of the predicted bubble score of the host application. The only guideline to designing a good reporter is to have a *broad sensitivity*, e.g. it should be sensitive to the memory subsystem holistically.

**[Designing the Reporter]** Like the bubble, there is also no *correct* design for the reporter. However, unlike the bubble, there is more flexibility in designing the reporter. This flexibility comes from the fact that the reporter is trained, and the sensitivity curve serves as a rubric for score reporting, no matter the shape. To implement the reporter, we use a mixture of random accesses and streaming accesses similar to those used for the bubble itself, without the high ILP. The working set of the reporter is about 20MB, thus it uses the last level cache, memory bandwidth and prefetcher.

Before the reporter can be used, it must first be trained using the bubble on the architecture for which it will be reporting. This training involves running the reporter against the bubble on the architecture of interest, and collecting the sensitivity curve of the reporter. This needs to be done only once. The reporter can then use its own sensitivity curve to translate a performance degradation it suffers to the corresponding bubble score. The curve is essentially used in

| workload             | description  | type              | metric           |
|----------------------|--|-------------------|------------------|
| bigtable             | A distributed storage system for managing petabytes of structured data   | latency-sensitive | user time (secs) |
| ads-servlet          | Ads sever responsible for selecting and placing targeted ads on syndication partners sites   | latency-sensitive | cpu latency (ms) |
| maps-detect-face     | Face detection for streetview automatic face blurring  | batch             | user time (secs) |
| maps-detect-lp       | OCR and text extraction from streetview  | batch             | user time (secs) |
| maps-stitch          | Image stitching for streetview   | batch             | user time (secs) |
| <b>search-render</b> | Web search frontend server, collect results from many backends and assembles html for user.  | latency-sensitive | user time (secs) |
| search-scoring       | Web search scoring and retrieval (traditional)   | latency-sensitive | queries per sec  |
| nlp-ml-train         | Language translation   | latency-sensitive | user time (secs) |
| openssl              | Secure Sockets Layer performance stress test.  | latency-sensitive | user time (secs) |
| protobuf             | Protocol Buffer, a mechanism for describing extensible communication protocols and on-disk structures. One of the most commonly-used programming abstractions at Google. | latency-sensitive | aggregated       |
| docs-analyzer        | Unsupervised Bayesian clustering tool to take keywords or text documents and "explain" them with meaningful clusters.  | both              | throughput       |
| docs-keywords        | Unsupervised Bayesian clustering tool to take keywords or text documents and "explain" them with meaningful clusters.  | both              | throughput       |
| rpc-bench            | Google rpc call benchmark  | both              | throughput       |
| saw-countw           | Sawzall scripting language interpreter benchmark   | both              | user time (secs) |
| goog-retrieval       | Web indexing   | batch             | ms per query     |
| youtube-x264yt       | x264yt video encoding.   | batch             | user time (secs) |
| zippy-test           | A lightweight compression engine designed for speed over space.  | both              | user time (secs) |

Table 1: Production Datacenter Applications

reverse. Instead of using scores to predict QoS, we use the QoS of the reporter to ascertain the score of the co-located application.

## 4. LARGE-SCALE WSC WORKLOADS

In this section, we present the large-scale datacenter application workloads used in this work, and characterize their susceptibility to performance interference due to contention for the shared memory subsystem resources. We also introduce **SmashBench**, our in house benchmark suite for the characterization of performance interference.

### 4.1 Large-Scale Data Intensive Workloads

While a large portion of the world’s computation is housed in the cloud, little is known about the application workloads that live in this computing domain. The characteristics of the tasks that compose a large scale web-service vary significantly. In addition to data retrieval tasks, there are compute-intensive tasks for the analysis, organization, scoring, and preparation of information for applications such as search, maps, ad serving, etc.

Table 1 presents a number of key application tasks housed in Google’s production datacenters. These application tasks comprise a majority of the CPU cycles in arguably the largest datacenter infrastructure in the world. In addition to each application task’s name, Table 1 shows the description, priority class, and key optimization metric for each workload. Each application task corresponds to an actual binary that is run in the datacenter. Application tasks that are user-facing, both directly and indirectly, are classified as *latency-sensitive* as the response time is paramount. Throughput oriented tasks that are not user-facing are classified as *batch*. Notice that some tasks may be used in both roles, and are denoted as *Both* in the table. The column marked *metric* shows the key metric for each application. In the context of this work, each task’s QoS is defined to be its performance along this metric.

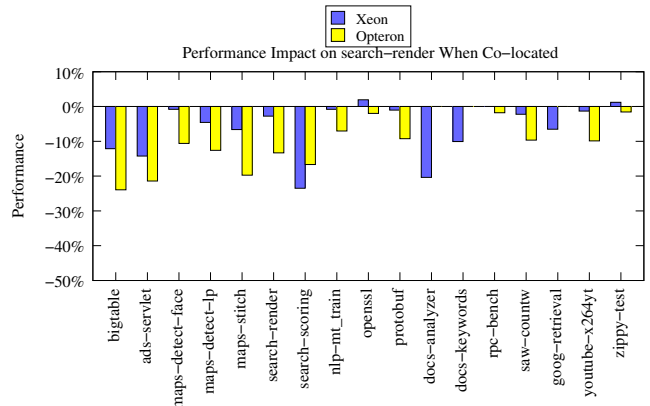


Figure 8: The performance degradation suffered by search-render when co-located with each of the other datacenter applications on Xeon and Opteron

We have highlighted **search-render** in Table 1. This task is responsible for assembling the final view of the search process for the user, which includes assembling scored search results (including web, image, and video), relevant ads from the ads-servlet, etc. This task is highly latency-sensitive and presents a compelling case that we use throughout this work to illustrate the necessity and value of Bubble-Up.

Figure 8 shows the performance degradation of **search-render** when co-located with the other application tasks shown in Table 1. This figure shows this performance interference on a production six-core Nehalem-based Xeon and a production six-core K10-based Opteron respectively. Each task in the co-location is configured to use three out of the six cores on the same socket of each platform. Note that **docs-analyzer**, **docs-keywords** and **goog-retrieval** do not have a data point for the Opteron. These particular

| kernel         | access pattern                               | stress point    | w.s. size | type       |
|----------------|--|-----------------|-----------|------------|
| blockie-small  | Dense 3D Matrix Transformations              | cpu-bound       | 7KB       | streaming  |
| blockie-medium | Dense 3D Matrix Transformations              | cache           | 10MB      | streaming  |
| blockie-large  | Dense 3D Matrix Transformations              | bandwidth       | 46MB      | streaming  |
| bst-small      | Binary Search Tree Traversal                 | cache (partial) | 4MB       | structured |
| bst-medium     | Binary Search Tree Traversal                 | cache           | 8MB       | structured |
| bst-large      | Binary Search Tree Traversal                 | bandwidth       | 50MB      | structured |
| lfsr-small     | Linear Shift Feedback Register Random Access | cache (partial) | 4MB       | random     |
| lfsr-medium    | Linear Shift Feedback Register Random Access | cache           | 8MB       | random     |
| lfsr-large     | Linear Shift Feedback Register Random Access | bandwidth       | 50MB      | random     |
| naive-small    | STL Random Access                            | cache (partial) | 4MB       | random     |
| naive-medium   | STL Random Access                            | cache           | 8MB       | random     |
| naive-large    | STL Random Access                            | bandwidth       | 50MB      | random     |
| sledge1        | Streaming Sparse Matrix Operations           | cache           | 7MB       | streaming  |
| sledge2        | Streaming Sparse Matrix Operations           | bandwidth       | 42MB      | streaming  |
| sledge3        | Streaming Sparse Matrix Operations           | bandwidth       | 399MB     | streaming  |

**Table 2: SmashBench Suite (stress point assumes a last level cache size of 6MB to 12MB)**

workloads must be run on the Xeon platform as they have been specially configured for this platform. As shown in the figure, we observe a significant amount of cross-core interference. This has led to a policy to disallow the co-location of `search-render` and other tasks on the same machine. However, some co-locations result in minimal to no interference. With the ability to precisely predict the performance interference suffered, those co-locations can be identified as safe, and the utilization of idle cores can be reclaimed.

## 4.2 SmashBench: Performance Interference Benchmark Suite

It is also important to note that various applications generate contention with various access patterns and working set sizes, which results in differing amounts of pressure across shared resources such as on-chip caches and buses to main memory. To characterize the sensitivity of our large-scale datacenter workloads to a spectrum of contention types, and to properly evaluate the effectiveness of Bubble-Up for predicting the performance interference that results from these various types of contention, we have created an in-house benchmark suite of contentious kernels, which we call **SmashBench**.

Table 2 shows the various kernels in our SmashBench suite. This suite of contentious workloads were designed specifically to exercise the resources that lie between the cores of a multicore processor and main memory in a spectrum of access patterns and working set sizes. As shown in the figure, SmashBench spans five access patterns. Each pattern continuously performs memory operation on a chunk of memory, which is of the size denoted *w.s. size*. The *stress point* of each application is either the shared on-chip caches or the bandwidth to memory, which is primarily a function of its working set size. Note that this instance of the suite assumes a last level cache size of approximately 6MB to 12MB. Current production datacenter deployments house processors with these specifications. It is important to note that while this version of the suite was designed for the platforms used in current production datacenters, it can be easily extended for future processor designs by modifying the working set size.

## 5. EVALUATION

In this section, we evaluate both 1) the accuracy of Bubble-Up in precisely predicting performance degradations due to interference, and 2) the effectiveness of leveraging Bubble-Up to improve utilization in a production datacenter environment.

The primary platform used in our evaluation is a six-core Nehalem-based Xeon. The performance metric used to describe the QoS of each Google application is the internal metric as presented in Table 1. Each application task is configured to use three cores on the six-core machines and two cores on the quad-core machines. As previously described, during the characterization phase, the bubble runs on the remaining cores.

### 5.1 Sensitivity Curves of WSC Workloads

We first present the sensitivity curves for Google benchmarks generated by our Bubble-Up methodology. The goal is to 1) examine our Bubble-Up design through analyzing the resulted sensitivity curves and 2) to further improve our understanding of how pressure in the shared resources affects the QoS of Google’s applications. To generate sensitivity curves, we adjust the pressure Bubble-Up generates and measure an application’s QoS under each given pressure. Figures 9 to 17 present the sensitivity curve of each Google application. For each figure, the x-axis shows the pressure on the shared memory system generated using Bubble-Up’s bubble. The y-axis shows the QoS performance of each application, normalized by its performance when it is running alone on the platform.

#### 5.1.1 Bubble Design

Figures 9 to 17 illustrate that our bubble design does indeed have the three properties described in Section 3.3. We observe *Monotonic Curves*. In general, each application’s QoS is decreasing as the pressure increases. This confirms our hypothesis that we can create an aggregate pressure “dial” in software that negatively and monotonically impacts an application’s QoS. We also observe *Wide Dial Range*. The sensitivity curves generally flatten after the Bubble-Up pressure goes beyond 20MB. At this point, the pressure on the shared cache and memory bandwidth saturates and further increase of the pressure would not have much more impact on an application’s QoS. Finally, we observe *Broad*

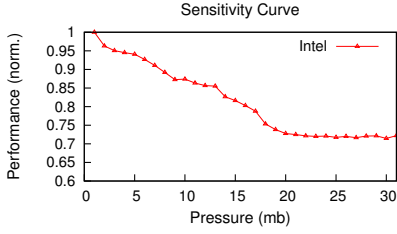


Figure 9: bigtable

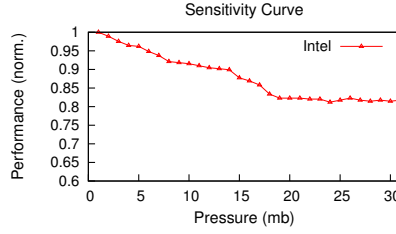


Figure 10: ads-servlet

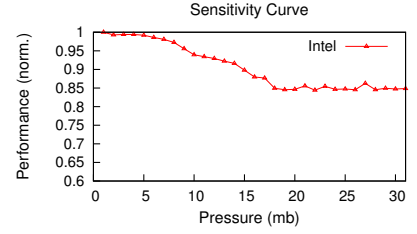


Figure 11: maps-detect-face

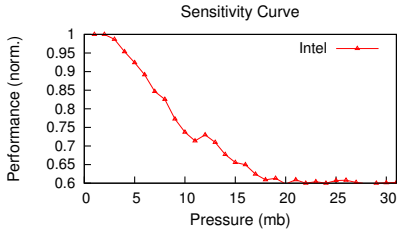


Figure 12: search-render

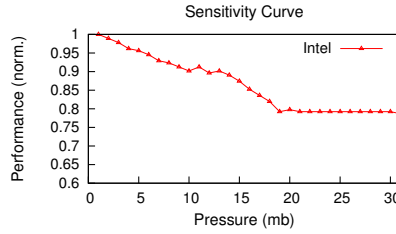


Figure 13: search-scoring

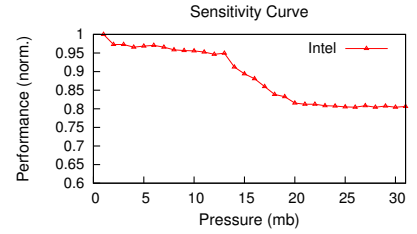


Figure 14: protobuf

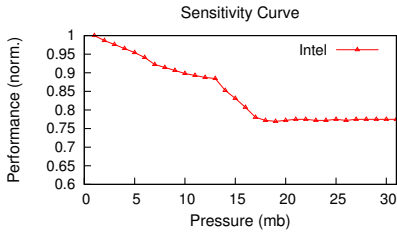


Figure 15: docs-analyzer

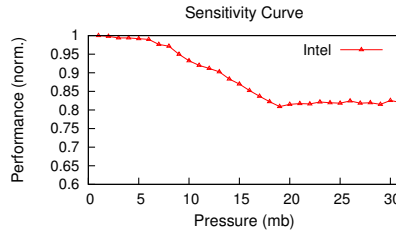


Figure 16: saw-countw

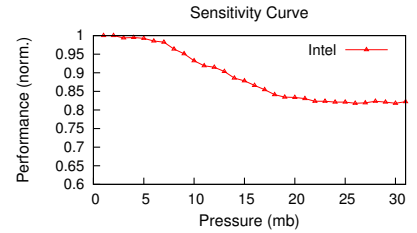


Figure 17: youtube-x264yt

*Impact.* The monotonic trend beyond 12MB shows that we are not only saturating the cache, but also the bandwidth to memory. The pressure generated by the bubble stresses the caches, bandwidth and prefetchers (due to streaming behavior described in Section 3.3).

### 5.1.2 Workload Characteristics

Some curves (e.g., `search-render`) are decreasing more sharply than others (e.g., `protobuf`). Also, at a given pressure point, each application suffers a different amount of QoS degradation. For example, at pressure point 10, `search-render`'s normalized QoS is only 0.7, while `protobuf`'s QoS is still around 0.95. When the curve flattens, each application's plateau QoS is also different, ranging from 0.6 to 0.85. This shows that Google applications' QoS have different levels of sensitivity to the pressure in the shared resources. Also, each application's sensitivity to various resources may be different. Since the experimental platform has a 12MB last level cache, the pressure before 12MB is only applied on the shared cache, and after 12MB, the pressure is applied on both shared cache and memory bandwidth. Comparing the gradients of an application's curve before and after 12 MB can help gain insights on its sensitivity to various resources. For example, `protobuf`'s curve is fairly flat before 12 MB but has a steep dip after 12MB. This indicates that `protobuf`'s QoS may be more sensitive to the pressure on the memory bandwidth than the shared cache.

## 5.2 Bubble Up Prediction Accuracy

In this section, we evaluate Bubble-Up's accuracy when predicting the QoS degradation of the applications due to performance interference.

### 5.2.1 Co-locating Google with SmashBench

We first evaluate the effectiveness of Bubble-Up in predicting the impact of our SmashBench workloads on Google's applications. In this experiment, we apply step one of our methodology to 9 memory intensive Google applications, and step two to our 15 SmashBench workloads. As previously mentioned, step one needs only to be applied to applications whose QoS needs to be enforce. Step two only needs to be applied to the applications that may threaten an application's QoS. Figure 18 to 26 present the results for each of the 9 Google applications. For each figure, the x-axis shows each of the 15 SmashBench benchmarks. The y-axis shows the Google application's QoS degradation. For each benchmark on the x-axis, the first bar shows the Google application's predicted degradation when co-located with the benchmark; the second bar is its measured degradation. The closer the two bars are, the more accurate the Bubble-Up prediction is. Each figure's caption also documents the average prediction error for each Google application, calculated using the absolute difference between the prediction and the measured value. In general, Bubble-Up's prediction error is quite small. For the nine Google applications, the pre-



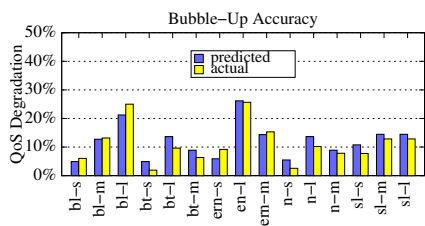


Figure 18: bigtable, avg. error - 2.2%

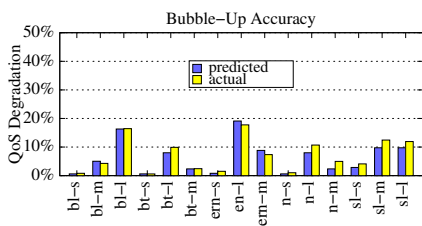


Figure 19: ads-servlet, avg. error - 0.8%

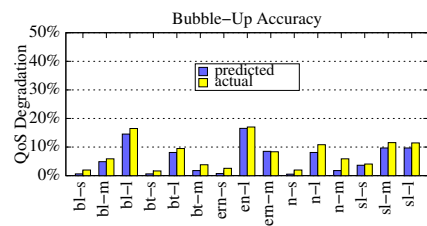


Figure 20: maps-detect-face, avg. error - 0.7%

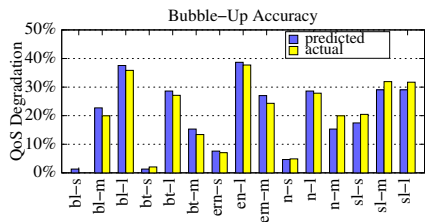


Figure 21: search-renderer, avg. error - 1.8%

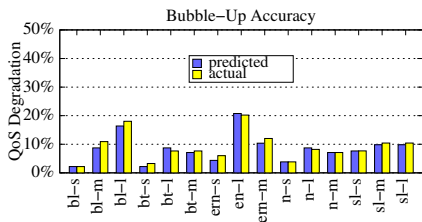


Figure 22: search-scoring, avg. error - 0.8%

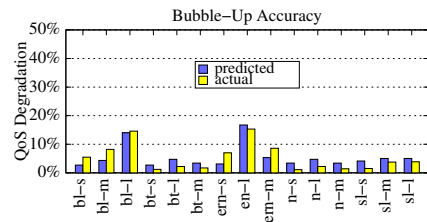


Figure 23: protobuf, avg. error - 2.2%

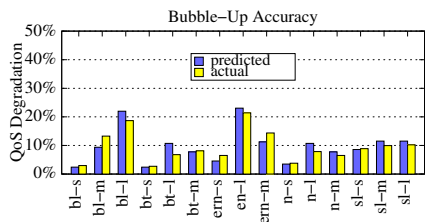


Figure 24: docs-analyzer, avg. error - 1.7%

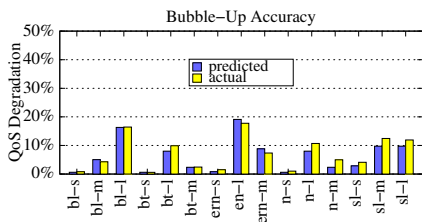


Figure 25: saw-count2, avg. error - 1.2%

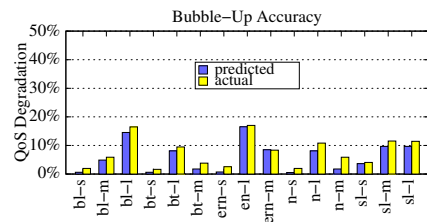


Figure 26: youtube-x264yt, avg. error - 1.5%

diction error is 2.2% or less. SmashBench exhibits a wide range of memory access patterns, stress points and working set sizes. The fact that a single Bubble-Up design can predict accurately the QoS degradation caused by SmashBench demonstrates the generality of the Bubble-Up methodology.

### 5.2.2 Pairwise Google Co-location

Figure 27 summarizes the prediction accuracy of Bubble-Up for pairwise co-locations with nine of the most sensitive Google applications with the complete set of Google applications (shown in the x-axis). Each bar shows the error (delta) between the performance degradation predicted by Bubble-Up and the actual measured performance degradation in the co-location. Errors in the negative direction imply that the actual QoS degradation is worse (more) than predicted; errors in the positive direction implies that the actual QoS degradation is better (less) than predicted. Only errors in the negative direction can result in a violation of a QoS policy. As the figure shows, Bubble-Up’s prediction error is fairly small across all Google pairwise co-locations.

## 5.3 Applying Bubble-Up in the Datacenter

In this section, we present an evaluation of applying Bubble-Up’s QoS prediction to increase co-location and machine utilization in datacenters. To predict the performance degradation on an application  $A$  when co-located with  $B$ , we use  $B$ ’s bubble score to index into  $A$ ’s sensitivity curve. To

improve machine utilization, we allow latency-sensitive applications to have a small amount of QoS degradation. The tolerable degradation threshold is specified in a QoS policy (Section 2). Using Bubble-Up, we can predict the QoS degradation and allow co-location of latency-sensitive applications with other applications when the predicted QoS degradation is within the specified threshold. To evaluate the effectiveness of Bubble-Up, we constructed a scenario where we evaluate 1) the machine utilization improvement when using Bubble-Up; and 2) the success of Bubble-Up’s prediction in satisfying a QoS policy without violating the specified QoS threshold.

For the production scenario presented in this section, we conducted our evaluation using a cluster that is composed of 500 machines, described in Section 5. In this experiment, we focused on **search-render** as our main latency-sensitive application whose QoS degradation must be limited within a small amount. In this cluster, there are 500 instances of **search-render**, each placed on a single machine. There are 500 other Google applications, evenly distributed across 15 application types shown in Table 1. Every application uses three cores. Our evaluation baseline is the currently deployed cluster management that disallows co-location of **search-render** with any other applications. In this experiment, we investigated the potential co-location and utilization gained using Bubble-Up predictions under varying QoS policies.

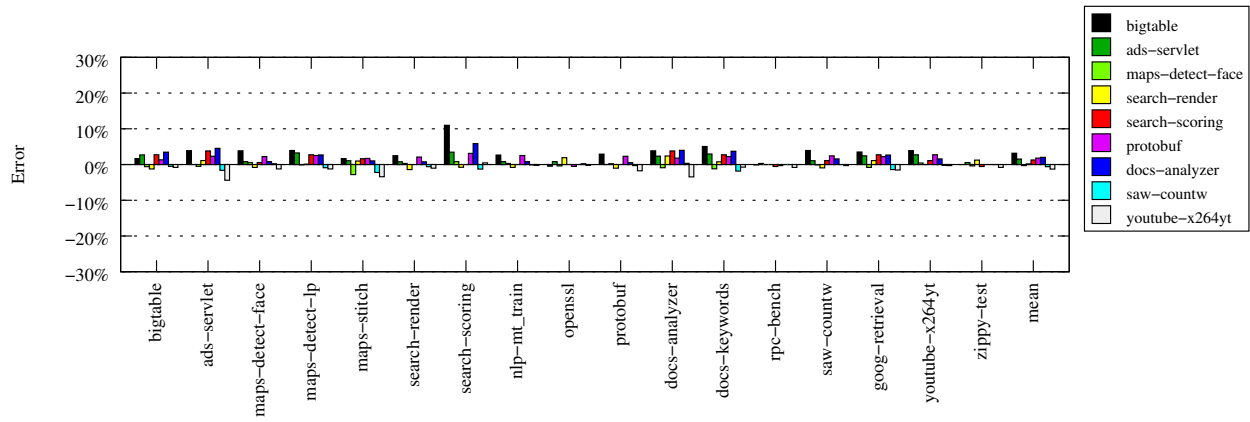


Figure 27: Bubble-Up's predication accuracy for pairwise co-locations of Google applications.

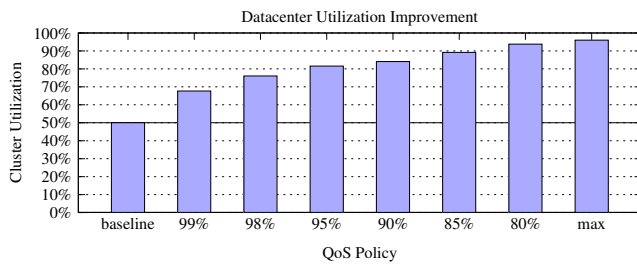


Figure 28: Improvement in cluster utilization when allowing Bubble-Up co-locations with search-render under each QoS policy.

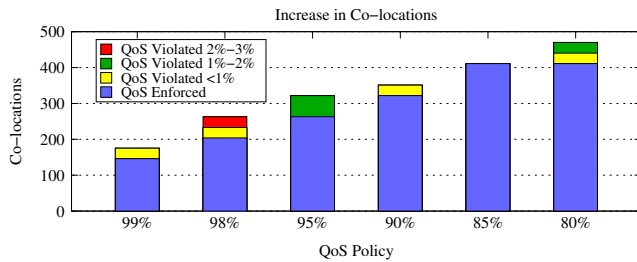


Figure 29: Number of Bubble-Up co-locations under each QoS policy.

Figure 28 presents the cluster's utilization achieved by Bubble-Up prediction under various QoS policies. The baseline is the utilization of the cluster when co-location is disallowed and each instance of `search-render` is occupying three out of the six cores on a single machine, and thus at 50% cluster utilization. The max utilization is achieved by allowing all co-locations; placing each of all 500 other Google applications to co-run with a `search-render` on every machine, regardless of `search-render`'s QoS degradation. The max utilization is not 100% because we define a machine's utilization as the aggregate performance of all applications running on the machine, normalized by their solo performance. For example, application *A* and *B* are co-locating and occupying all six cores on a machine, but due to cross-core interference, their performance is only 90% of that when running alone occupying three cores on a machine. Then the

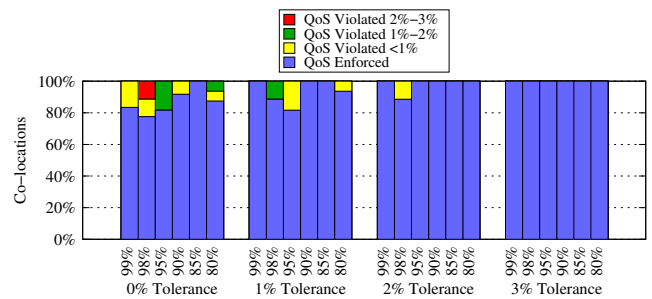
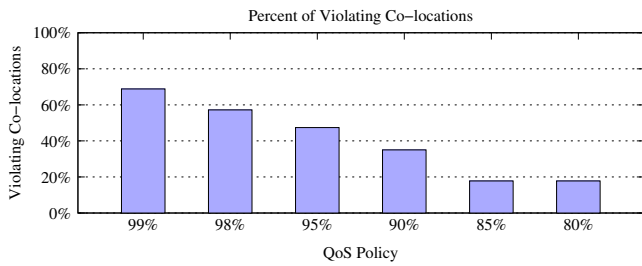


Figure 30: Reduction in QoS violations when applying a tolerance to each QoS policy. Having a tolerance of just a few percent results in no violations.

machine utilization when co-located is only 90% instead of 100%.

As Figure 28 demonstrates, Bubble-Up prediction greatly improves machine utilization. Even under 99% of QoS policy (when the tolerable QoS degradation is only 1%), the utilization is improved from 50% to close to 70%. Allowing a more relaxed QoS policy improves the utilization even more. Under 80% QoS policy, the utilization improvement is close to 80%, showing great potential benefit of adopting Bubble-Up in datacenters.

Figure 29 presents the total number of co-locations allowed by the cluster manager according to Bubble-Up prediction under each QoS policy. Similar to utilization, the number of co-location increases as the allowed QoS degradation increases. The baseline co-location is 0. With 99% QoS policy, the co-location is close to 200. With 80% QoS policy, the allowed co-locations increase to 400. However, because of Bubble-Up's prediction error, there may be co-locations that violate the QoS threshold specified in the policy. Both the number of co-locations that satisfy the QoS policy and the number of violations are presented in stack bars. The violations are broken down into three categories: violations that cause less than 1% extra degradation beyond the QoS policy, 1-2% extra degradation and 2-3% degradation. For example, as shown in the figure, under 99% QoS policy, around 10% of the co-locations violate the policy. However, all of these violations only cause less than 1% extra QoS degradation beyond the policy, meaning their QoS is within a 98% QoS policy. Figure 30 shows the effect of



**Figure 31: QoS violations when allowing all 500 co-locations with search-render under each QoS policy. (Random Assignment)**

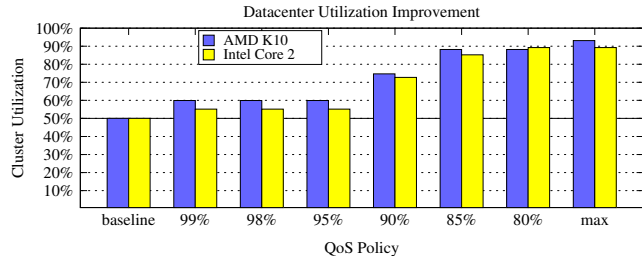


**Figure 32: Improved utilization in a clusters composed of AMD K10 Opteron servers and Intel Core 2 Xeon servers.**

updating the QoS policy to include an error *tolerance*. As shown in the figure, increasing error tolerance at each QoS policy reduces the number of violations. Note that most of the violations cause only less than 2% of extra QoS degradation beyond the QoS policy. Figure 31 shows the percentage of violating co-locations when allowing all co-locations for each QoS policy.

## 5.4 Impact of Varying Architecture

To evaluate the generality of our Bubble-Up across microarchitectures, we conducted similar experiments on two additional platforms (a six-core K10-based Opteron and a four-core Core2-based Xeon) with the same bubble and reporter used on the Nehalem processor. The experimental setup is similar as Section 5.3. Figure 32 demonstrates the utilization improvement for the cluster when using Bubble-Up prediction for a cluster composed of Opteron and a cluster composed of Core2-based Xeons. As Figure 33 shows, Bubble-Up can effectively increase the number of co-locations with a small amount of error on both platforms. The platforms presented here both have a smaller shared cache sizes and lower bandwidth than the Nehalem processor. This leads to a higher degree of contention on these processors. As a result, we observe fewer co-locations at higher QoS policy thresholds. At the 90% threshold the number of co-locations allowed increases dramatically.

## 6. RELATED WORK

While there has been a lot of work on mitigating the performance interference due to resource contention on multi-core, not much work is directly applicable to the datacenter co-location problem. Perhaps the closest related work is the Quarta work by Govindan et al. [9]; however this work requires access to physical memory addresses which can only be attained via custom changes to the OS, and

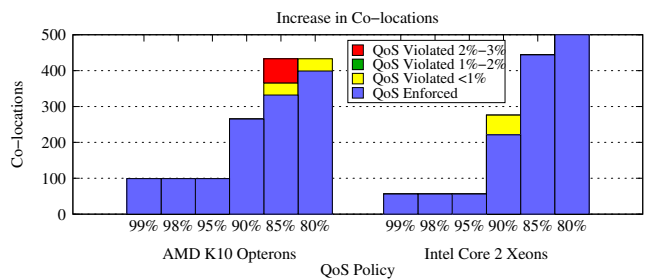


**Figure 33: Co-locations allowed in Opteron and Xeon clusters.**

as the authors themselves mention, such an approach is not feasible at user-level. One direction that has attracted much research attention is the management of shared cache and bandwidth through techniques such as resource partitioning [4, 20, 27–34, 38], throttling [7] and adaptive cache replacement policies [14]. Previous work has also investigated providing QoS management for different applications on multicore [10, 11, 13, 26]. While demonstrating promising results, the previous work on QoS management and resource partitioning typically requires changes to the hardware design, which is not applicable to deployed servers. Software resource partitioning has also been proposed [6, 19, 35]. However, most software partitioning techniques focus on shared cache, while ignoring memory bandwidth contention, which is another main cause of performance interference. In general, our work is complementary to the above resource management research. While previous work focuses on providing resource management for performance isolation or performance optimization for co-running applications, our work focus on predicting which applications can be co-run with a given application without degrading its QoS beyond a certain threshold.

Previous work on scheduling to mitigate contention and to improve cache sharing is closely related to our work [5, 8, 16, 17, 40]. For an application, different co-runners may cause different amounts of performance interference on a CMP. The intuition of many contention-aware scheduling is to classify applications based on how aggressively they are for shared memory resources and intelligently matches highly aggressive applications with not aggressive applications to minimize the performance degradation [16, 17, 41]. However, most previous work focuses on maximizing the overall throughput or maintaining performance fairness. The approaches cannot address challenges when applications have different priorities and a subset of the applications have strict requirements in terms of the tolerable QoS degradation. The challenge for scheduling to provide such QoS guarantee is that the scheduler needs to accurately predict the potential performance degradation for co-running applications. Current classifiers in contention-aware schedulers only indirectly classify or rank applications in terms of their levels of aggressiveness [17, 37, 41] or predict their potential cache misses [3, 16, 21], but cannot provide direct accurate prediction in terms of performance degradation.

## 7. CONCLUSIONS

In this work, we have presented a novel methodology for the precise prediction of the performance degradation that results from contention for shared resources. This mechanism is of particular importance in the emerging domain of

warehouse scale computing. By decoupling the characterization of an application’s sensitivity to contentious pressure to the memory subsystem, and the pressure it generates in the subsystem, we are able to predict pairwise co-locations with only a 1% prediction error on average. Using Bubble-Up in our experimental cluster setup, we are able to increase the utilization in the datacenter by 50% to 90% while enforcing a range of QoS policies.

## 8. ACKNOWLEDGEMENTS

We would like to thank Dick Sites, Silvius Rus, and Rick Hank for their invaluable feedback. We would also like to thank Neil Vachharajani for his healthy skepticism and keeping us on our toes. Finally, we would like to thank the reviewers for their feedback and suggestions. Jason Mars is supported by a Google Ph.D. fellowship. This work was partially supported by Google and NSF grant 0811689 to the University of Virginia.

## 9. REFERENCES

- [1] G. Banga, P. Druschel, and J. C. Mogul. Resource containers: a new facility for resource management in server systems. In *OSDI '99*, Berkeley, CA, USA, 1999. USENIX Association.
- [2] L. A. Barroso and U. Hözl. The case for energy-proportional computing. *IEEE Computer*, 40:33–37, December 2007.
- [3] D. Chandra, F. Guo, S. Kim, and Y. Solihin. Predicting inter-thread cache contention on a chip multi-processor architecture. In *HPCA '05*, pages 340–351, Washington, DC, USA, 2005. IEEE Computer Society.
- [4] J. Chang and G. Sohi. Cooperative cache partitioning for chip multiprocessors. *Supercomputing*, page 252, 2007.
- [5] S. Chen, P. Gibbons, M. Kozuch, V. Liaskovitis, A. Ailamaki, G. Blueloch, B. Falsafi, L. Fix, N. Hardavellas, T. Mowry, and C. Wilkerson. Scheduling threads for constructive cache sharing on cmps. *SPAA '07*, Jun 2007.
- [6] S. Cho and L. Jin. Managing distributed, shared l2 caches through os-level page allocation. *MICRO 39*, Dec 2006.
- [7] E. Ebrahimi, C. Lee, O. Mutlu, and Y. Patt. Fairness via source throttling: a configurable and high-performance fairness substrate for multi-core memory systems. *ASPLOS '10*, 2010.
- [8] A. Fedorova, M. Seltzer, and M. Smith. Improving performance isolation on chip multiprocessors via an operating system scheduler. *PACT '07*, Sep 2007.
- [9] S. Govindan, J. Liu, A. Kansal, and A. Sivasubramaniam. Cuanta: Quantifying effects of shared on-chip resource interference for consolidated virtual machines. In *SOCC '11*, Oct 2011.
- [10] F. Guo, Y. Solihin, L. Zhao, and R. Iyer. A framework for providing quality of service in chip multi-processors. *MICRO 40*, Dec 2007.
- [11] A. Herdrich, R. Illikkal, R. Iyer, D. Newell, V. Chadha, and J. Moses. Rate-based qos techniques for cache/memory in cmp platforms. *ICS '09*, Jun 2009.
- [12] U. Hoelzle and L. A. Barroso. *The Datacenter as a Computer: An Introduction to the Design of Warehouse-Scale Machines*. Morgan and Claypool Publishers, 1st edition, 2009.
- [13] R. Iyer, L. Zhao, F. Guo, R. Illikkal, S. Makineni, D. Newell, Y. Solihin, L. Hsu, and S. Reinhardt. Qos policies and architecture for cache/memory in cmp platforms. *SIGMETRICS '07*, Jun 2007.
- [14] A. Jaleel, W. Hasenplaugh, M. Qureshi, J. Sebot, S. Steely, Jr, and J. Emer. Adaptive insertion policies for managing shared caches. *PACT '08*, Oct 2008.
- [15] V. Janapa Reddi, B. C. Lee, T. Chilimbi, and K. Vaid. Web search using mobile cores: quantifying and mitigating the price of efficiency. In *ISCA '10*, New York, NY, USA, 2010. ACM.
- [16] Y. Jiang, K. Tian, and X. Shen. Combining locality analysis with online proactive job co-scheduling in chip multiprocessors. *HiPeac '10*, pages 201–215, 2010.
- [17] R. Knauerhase, P. Brett, B. Hohlt, T. Li, and S. Hahn. Using os observations to improve performance in multicore systems. *IEEE Micro*, 28:54–66, May 2008.
- [18] C. Kozyrakis, A. Kansal, S. Sankar, and K. Vaid. Server engineering insights for large-scale online services. *IEEE Micro*, 30, July 2010.
- [19] J. Lin, Q. Lu, X. Ding, Z. Zhang, X. Zhang, and P. Sadayappan. Gaining insights into multicore cache partitioning: Bridging the gap between simulation and real systems. *HPCA '08*, pages 367–378, 2008.
- [20] F. Liu, X. Jiang, and Y. Solihin. Understanding how off-chip memory bandwidth partitioning in chip multiprocessors affects system performance. *HPCA '10*, pages 1–12, 2010.
- [21] J. Machina and A. Sodan. Predicting cache needs and cache sensitivity for applications in cloud computing on cmp servers with configurable caches. *IPDPS 2009*, pages 1 – 8, 2009.
- [22] J. Mars, L. Tang, and R. Hundt. Heterogeneity in “homogeneous” warehouse-scale computers: A performance opportunity. *IEEE Computer Architecture Letters*, 2011.
- [23] J. Mars, L. Tang, and M. L. Soffa. Directly characterizing cross-core interference through contention synthesis. In *HiPEAC '11*, pages 167–176, New York, NY, USA, 2011. ACM.
- [24] J. Mars, N. Vachharajani, R. Hundt, and M. L. Soffa. Contention aware execution: online contention detection and response. In *CGO '10*, New York, NY, USA, 2010. ACM.
- [25] A. Mishra, J. Hellerstein, W. Cirne, and C. Das. Towards characterizing cloud backend workloads: insights from google compute clusters. *ACM SIGMETRICS Performance Evaluation Review*, 37(4):34–41, 2010.
- [26] M. Moreto, F. Cazorla, A. Ramirez, R. Sakellariou, and M. Valero. Flexdcp: a qos framework for cmp architectures. *SIGOPS Operating Systems Review*, 43(2), Apr 2009.
- [27] K. Nesbit, N. Aggarwal, J. Laudon, and J. Smith. Fair queuing memory systems. *MICRO-39*, pages 208 – 222, 2006.
- [28] K. Nesbit, M. Moreto, F. Cazorla, A. Ramirez, M. Valero, and J. Smith. Multicore resource management. *Micro, IEEE*, 28(3):6 – 16, 2008.
- [29] M. Qureshi and Y. Patt. Utility-based cache partitioning: A low-overhead, high-performance, runtime mechanism to partition shared caches. *MICRO 39*, Dec 2006.
- [30] N. Rafique, W.-T. Lim, and M. Thottethodi. Architectural support for operating system-driven cmp cache management. *PACT '06*, Sep 2006.
- [31] N. Rafique, W.-T. Lim, and M. Thottethodi. Effective management of dram bandwidth in multicore processors. *PACT 2007*, pages 245 – 258, 2007.
- [32] S. Srikantaiah, R. Das, A. Mishra, C. Das, and M. Kandemir. A case for integrated processor-cache partitioning in chip multiprocessors. *SC '09*, Nov 2009.
- [33] S. Srikantaiah, M. Kandemir, and M. Irwin. Adaptive set pinning: managing shared caches in chip multiprocessors. *ASPLOS XIII*, Mar 2008.
- [34] G. E. Suh, S. Devadas, and L. Rudolph. A new memory monitoring scheme for memory-aware scheduling and partitioning. In *HPCA '02*. IEEE Computer Society, 2002.
- [35] D. Tam, R. Azimi, L. Soares, and M. Stumm. Rapidmrc: approximating l2 miss rate curves on commodity systems for online optimizations. *ASPLOS '09*, Feb 2009.
- [36] L. Tang, J. Mars, N. Vachharajani, R. Hundt, and M. L. Soffa. The impact of memory subsystem resource sharing on datacenter applications. In *ISCA '11*, pages 283–294, New York, NY, USA, 2011. ACM.
- [37] Y. Xie and G. Loh. Dynamic classification of program memory behaviors in cmps. *Proc. of CMP-MSI, held in conjunction with ISCA-35*, 2008.
- [38] Y. Xie and G. Loh. Pipp: promotion/insertion pseudo-partitioning of multi-core shared caches. *ISCA '09*, Jun 2009.
- [39] C. Xu, X. Chen, R. Dick, and Z. Mao. Cache contention and application performance prediction for multi-core systems. In *ISPASS 2010*, march 2010.
- [40] D. Xu, C. Wu, and P.-C. Yew. On mitigating memory bandwidth contention through bandwidth-aware scheduling. *PACT '10*, Sep 2010.
- [41] S. Zhuravlev, S. Blagodurov, and A. Fedorova. Addressing shared resource contention in multicore processors via scheduling. *ASPLOS '10*, Mar 2010.